



IXPE Highly Significant Detection of Polarization in Scorpius X-1

Fabio La Monaca

on behalf of the [IXPE Science Team](#)

fabio.lamonaca@inaf.it

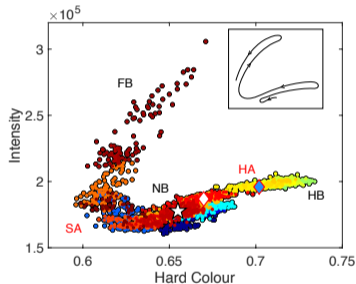
INAF-IAPS, Rome, Italy

La Monaca F., Di Marco A., Poutanen, J. et al.

[ApJL 960, L11, 2024](#)

preprint [arXiv:2311.06359](#)





[Motta & Fender, MNRAS, 483:3686 (2019)]

- First extra-solar X-ray source discovered and the brightest in the X-ray sky
- NS-LMXB with peak luminosity near the Eddington-limit for a $1.4 M_{\odot}$
- First X-ray binary where radio emission was detected:
 - ➔ VLBI observations spatially resolved **radio jet** at a position angle of $\sim 54^{\circ}$ (from north to east), deriving the inclination of the system: $44^{\circ} \pm 6^{\circ}$ (Fomalont et al., 2001)
- This is a prototype for Z-sources: usually divided in Sco-like and Cyg-like
- An ideal candidate to **attempt to measure X-ray polarization**: **OSO-8** satellite (Long et al., 1979) and **PolarLight** (Long et al., 2022)

■ Polarization can help to study "corona" geometry

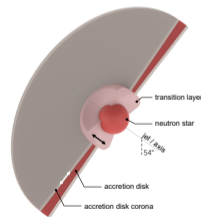
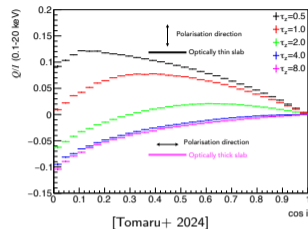
- Accretion disk PA expected parallel to the disk and perpendicular to the radio-jet
- SL/BL PA expected parallel or perpendicular to the disk depending on τ (Sunyaev & Titarchuk, 1985; Tomaru+ 2024)

■ In 1977, **OSO-8** (Long et al. 1979) obtained a low-significance detection at 2.6 keV and at 5.2 keV (PD = $1.3\% \pm 0.4\%$ and PA = $57^\circ \pm 6^\circ$ at $\sim 3\sigma$ CL)

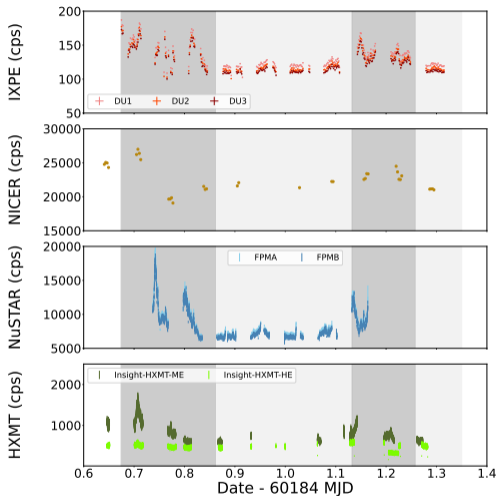
■ In 2022, **PolarLight** (Long et al., 2022) obtained hints of variations of polarization with the energy and the source flux:

- a 5σ detection (PD $\sim 4\%$) **only in the 4–8 keV energy band and when the flux was high with a PA aligned with the radio jet**

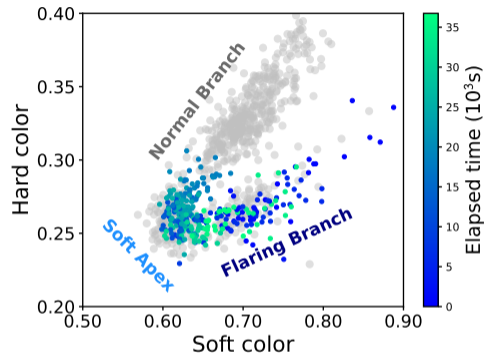
■ Both these observations were **performed with long exposure (~ 15 d for OSO-8 and ~ 322 d for PolarLight)**, and none of them could clearly distinguish the source state



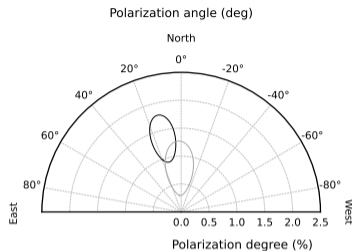
[Long+ 2022]



■ Flaring activity highlighted in dark gray

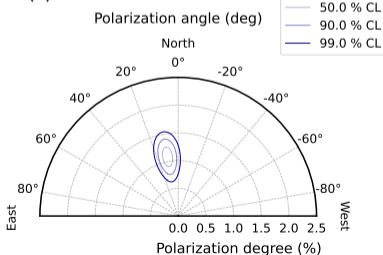


- NuSTAR Color–Color diagram: **observation mainly in SA with short periods in FB**
- NICER timing analysis: observed transient QPO at ~ 6 Hz **compatible with SA**

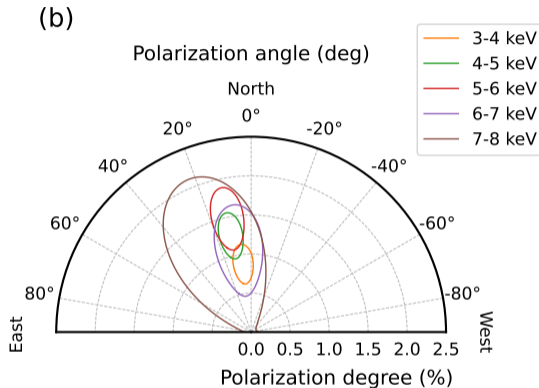
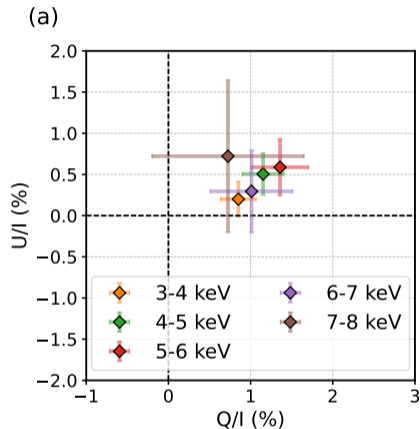


- Polarization for the flaring branch and non-flaring are **compatible within 90% CL**; thus, the analysis can be carried out on the entire observation

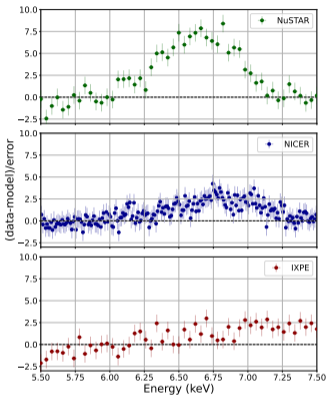
(c)



- **Secure detection** of polarization in 3-8 keV
 - probability of obtaining such polarization in the case of an unpolarized source is 6×10^{-12} , corresponding to a **detection significance of $\sim 7\sigma$ CL**.



- **No evidence of PD or PA variation with energy**
- All contours in the different 1 keV energy bins are compatible at 68% CL



Presence of a clear broad Fe line at ~ 6.7 keV observed in the data as a reflection feature

■ Spectral joint fit:

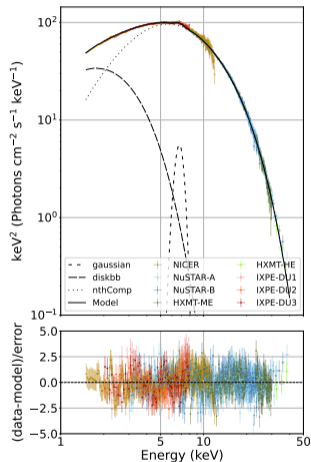
- NICER (1.5–12 keV) with SCORPEON background
- NuSTAR (3–40 keV)
- Insight-HXMT Medium Energy (ME) (8–20 and 23–30 keV) and High Energy (HE) telescopes (30–40 keV); Insight-HXMT Low Energy (LE) excluded from the analysis due to a reported calibration issue
- IXPE (2–8 keV)

■ Fit the continuum with:

- $\text{tbabs} * (\text{diskbb} + \text{nthcomp})$

■ $N_H = 0.15 \times 10^{22} \text{ cm}^{-2}$

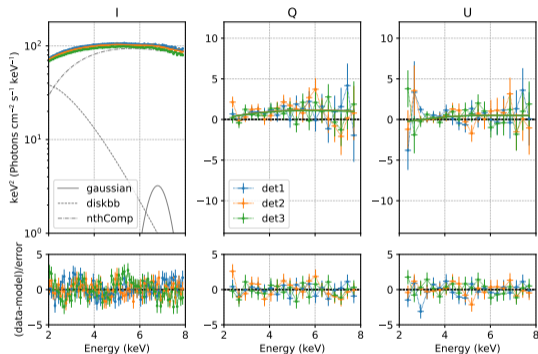
- `nthcomp` has `inp_type=0` corresponding to hot electrons Compton upscattering seed photons distributed as a blackbody, e.g., from the neutron star SL/BL



- Flux dominated by the Comptonization component

Component	Parameter	Continuum	Model A
tbabs	$N_{\text{H}} (\times 10^{22} \text{ cm}^{-2})$	0.15	0.15
diskbb	$kT_{\text{in}} \text{ (keV)}$	0.692 ± 0.004	0.683 ± 0.011
	norm $([R_{\text{in}}/D_{10}]^2 \cos \theta)$	25500 ± 700	25500 ± 1400
	$R_{\text{in}} \text{ (km)}$	40.1 ± 1.1	40.1 ± 2
nthcomp	Γ	2.78 ± 0.02	2.58 ± 0.02
	τ	5.95 ± 0.04	6.70 ± 0.05
	$kT_{\text{e}} \text{ (keV)}$	3.41 ± 0.03	3.21 ± 0.03
	$kT_{\text{bb}} \text{ (keV)}$	1.148 ± 0.008	1.08 ± 0.01
	norm	6.34 ± 0.05	6.94 ± 0.16
gauss	$E_{\text{line}} \text{ (keV)}$	-	6.72 ± 0.02
	$\sigma \text{ (keV)}$	-	0.45 ± 0.03
	norm $(\text{photon cm}^{-2} \text{ s}^{-1})$	-	0.139 ± 0.009
	Equivalent width (eV)	-	66.836 ± 0.014
		χ^2/dof	$5365/2890 = 1.9$ $3033/2887 = 1.05$
Photon flux ratios in 2-8 keV			
	$F_{\text{diskbb}}/F_{\text{tot}}$	0.23	0.21
	$F_{\text{nthcomp}}/F_{\text{tot}}$	0.77	0.78
	$F_{\text{gauss}}/F_{\text{tot}}$	-	0.01

- **tbabs*(gaussian+(diskbb+nthcomp)*polconst):**
 - PD = $1.0\% \pm 0.2\%$ and PA = $8^\circ \pm 6^\circ$
 - $\chi^2/\text{dof} = 1371/1341 = 1.02$
- **tbabs*(gaussian+(diskbb+nthcomp)*pollin):**
 - **no polarization varying linearly with energy:** PD and PA slopes compatible with zero



- The iron line is assumed to be unpolarized

Table 4. Best-fit parameters for the spectro-polarimetric analysis with the model `polconst*diskbb+polconst*nthcomp+gauss`.

Component		Value
diskbb	PD (%)	< 3.2
	PA (deg)	—
nthcomp	PD (%)	1.3 ± 0.4
	PA (deg)	14 ± 8
	χ^2/dof	$1329/1337 = 0.99$

NOTE—Errors are at 90% CL.

- Model C: $\text{tbabs} * (\text{diskbb} + \text{nthcomp} + \text{relxillNS})$
 - inclination frozen at 44° (Fomalont et al., 2001)
 - frozen Fe abundance and $\log N$ frozen to the maximum; similar effect seen for other bright sources, e.g. Cyg X-1 (Tomsick et al. ApJ, 855, 3, 2018)
 - relative flux for the reflection component at level of 10%

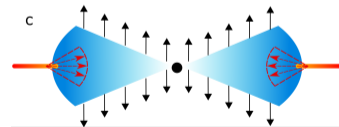
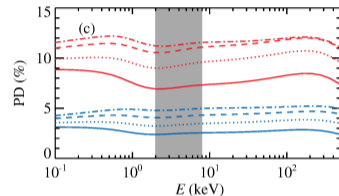
- Different constant polarization to each spectral component:

	Disk		Comptonization		Reflection	
Case A	$< 1.9\%$	–	$< 8.2\%$	–	$< 66\%$	–
Case B	1.1%	-40°	0%	–	$14\% \pm 5\%$	$15^\circ \pm 7^\circ$

- upper limits and errors at 90% CL

- **A clear polarimetric disentanglement of the three spectral components is not possible with the present data**

- **Highly significant polarization** in 2–8 keV energy band (PD=1.0%±0.2% and PA=8°±6°)
- **No evidence of PD or PA variation with the energy:** the **constant PD**, even if smaller than expectations, can be compatible with a **sandwich corona geometry** (Poutanen et al., ApJL 949:L10, 2023)
- PD of the disk **compatible with expectations from an electron-scattering dominated optically thick accretion disk** (Chandrasekhar, 1960) that is $\sim 1\%$ for an inclination $\sim 44^\circ$
- PD of the Comptonized component of $1.3\% \pm 0.4\%$, **compatible with the scenario of a coplanar corona having Thomson optical depth $\tau_T \sim 7$ and $kT_e \sim 3$ keV** as in Sunyaev & Titarchuk, 1985
- PD of the reflection component **compatible with the predicted polarization values for a Compton-reflected spectrum from cold matter** (Matt et al., 1993 and Poutanen et al., 1996).



- The present Sco X-1 measurement shows a PA rotated of $\sim 46^\circ$ with respect to the radio-jet position angle. In contrast with:

- ➔ previous OSO-8 and PolarLight attempts performed with long exposure times without branch selection/identification limiting their usefulness in the comparison
- ➔ IXPE results for Cyg X-2 (Farinelli+ 2023), Cyg X-1 (Krawczynski+ 2022)

- The IXPE measured PA may be due to relativistic precession or HR variations:

- ➔ **relativistic precession**: radio-jet observed in few sources to change up to 36° on short timescales (Miller-Jones+ 2019) likely related to the relativistic Lense-Thirring precession of the accretion disk; Observed also for NS: **evidence of precession of the radio-jet in Cir X-1** (F. Cowie, in preparation); this effect can produce a rotation of the PA if aligned with radio-jet with respect to previous measurements
- ➔ **variation of the corona geometry** in the different states of the source with PA variations up to $\sim 50^\circ$: see e.g., Cir X-1 (Rankin+ 2023) and GX 13+1 (Bobrikova+ 2024)
- ➔ **new Sco X-1 observations by IXPE** could try to answer this open question

- More details: La Monaca F., Di Marco A., Poutanen, J. et al. ([ApJL 960, L11, 2024](#))

